Photoelectron circular dichroism of isopropanolamine

D. Catone [a], S. Turchini [a,*], G. Contini [a], T. Prosperi [a], M. Stener [b,c], P. Decleva [b,c], N. Zema [a]

[a] Istituto Struttura della Materia, C.N.R., Via del Fosso del Cavaliere 100, 00133 Roma, Italy
[b] Dipartimento di Scienze Chimiche, Università di Trieste, Via L. Giorgieri 1, I-34127 Trieste, Italy
[c] Consorzio Interuniversitario Nazionale per la Scienza e Tecnologia dei Materiali, INSTM, Unita' di Trieste and INFM DEMOCRITOS National Simulation Center, Trieste, Italy

ARTICLE INFO

Article history:
Available online 6 September 2016

ABSTRACT

Spectroscopies based on circular polarized light are sensitive to the electronic and structural properties of chiral molecules. Photoelectron circular dichroism (PECD) is a powerful technique that combines the chiral sensitivity of the circular polarized light and the electronic information obtained by photoelectron spectroscopy. An experimental and theoretical PECD study of the outer valence and C 1s core states of 1-amino-2-propanol in the gas phase is presented. The experimental dichroic dispersions in the photoelectron kinetic energy are compared with theoretical calculations employing a multicentric basis set of B-spline functions and a Kohn-Sham Hamiltonian. In order to understand analogies and differences in the dichroism of structural isomers bearing the same functional groups, a comparison with previous PECD study of valence band of 2-amino-1-propanol is carried out.

1. Introduction

Investigation of chiral molecules has a strong impact in chemistry in various research areas, such as heterogeneous dissymmetric catalysis, photochemical asymmetric synthesis, enzymatic catalysis [1–4]. Although PhotoElectron Circular Dichroism (PECD) was predicted in 1976 [5], only in the last decade it has received an increasing attention in the study of electronic, structural and conformational properties of chiral molecules in the gas phase and it was first investigated on the valence band of bromocamphor [6] and on core levels of camphor [7]. Since a simple model to interpret the complex oscillating behavior of the dissymmetry dynamics as a function of photoelectron kinetic energy is unavailable, the comparison between experiment and theory is of primary importance. Theoretical approaches are reported in the literature, essentially based on MS-Xα [8] and DFT B-spline calculations [9]. The DFT B-spline calculation, employed in this work, produces an effective modeling of the experimental PECD dissymmetries for the valence band of methyloxirane [10,11], camphor [12], 3-hydroxytethrahydrofurane [13], alaninol [14] and 3-methylcyclopentanone [15]; moreover, the sensitivity to molecular conformation was proven for the C 1s core level of carvone [16] and glycidol [17], and for the valence band of glycidol [18], alaninol [14], 3-methylcyclopentanone [15]. The presence of positive/negative dissymmetry contributions in PECD, related to unresolved peaks in the photoelectron spectrum, allows to assign efficiently the molecular orbital character of electronic states [18,19]. PECD theoretical investigation [20] on methyl oxirane demonstrated how the effect of the rotation of methyl group can affect the shape and intensity of the dichroic dispersion as a function of photoelectron kinetic energy, showing the PECD sensitivity to slight deformation of the molecule. The PECD presents a new term, the dichroism parameter, in the angle resolved photoemission cross section. The dichroism parameter is present only in chiral molecules and arises from the interference of the l, l ± 1 outgoing partial wave. This term embodies the full information of phase difference between outgoing partial waves, whereas the classical photoionization parameters have no phase information (isotropic cross section) or partial l, l ± 2 (asymmetry parameter) [21]. The richer content in interference characterizes the sensitivity of the dichroism parameter to photoionization dynamics.

The electronic character of the molecular orbital in the initial state plays a valuable role in the oscillating shape of the dichroism dispersion, as well as the vibrational modes of the ionic final state [22,23]. PECD can show large variations across the vibrational features of the photoelectron spectra, revealing in a clear way violations of the Franck-Condon principle [24]. A theoretical comparison between oxirane derivatives [9] showed that the atom substitution meaningfully alters the dispersion of the dichroism as a function of the photoelectron kinetic energy. Moreover PECD can be related to electronic correlation effects by core levels resonance [25], opening new perspectives in the characterization of dissymmetric catalysts, such as metal-organic systems and biomolecules.

* Corresponding author.
E-mail address: stefano.turchini@ism.cnr.it (S. Turchini).

http://dx.doi.org/10.1016/j.chemphys.2016.09.004

Circular dichroism in the angular distribution in photoemission is also a valuable spectroscopy for surface science involving chiral supramolecular assemblies [26,27]. Recently, PECD spectroscopy with a multiphoton coincidence detection revealed a powerful analytical application providing fully multiplexed mass-tagged photoelectron circular dichroism spectra in multi-component mixtures of chiral molecules [28].

Herein we present the PECD study of 1-amino-2-propanol (isopropanolamine), a linear saturated bifunctional molecule with different conformations at room temperature. The isopropanolamine is a structural isomer of 2-amino-1-propanol (alaninol), with an exchanged position of the two functional groups (—OH, —NH_2) at chiral carbon on a similar skeleton structure. In this paper we directly relate previous photoelectron spectroscopy (PES) studies on alaninol and isopropanolamine [29] and the PECD investigation on the valence band of alaninol [14]. The study of molecules which share well definite electronic and structural properties can shed light on characteristic features of the photoelectron dichroism. Major features of the valence band photoelectron spectrum of isopropanolamine are reproduced well by the most abundant conformer, with the second conformer making a distinctive contribution to the PES profile only in the Ionization Energy (IE) region around 14.8 eV [29]. For alaninol the PECD valence band together with photoelectron spectra gave an effective modeling of the conformer assignment and of the molecular orbital electronic character [14]. The aim of this work is twofold: use PECD in complementing the PES spectra analysis for isopropanolamine and compare valence band PECD of isopropanolamine and alaninol to find correspondences and differences, relating them to the molecular orbital character of the two chiral isomers.

2. Experimental details

The experiment was performed at the "Circular Polarization" 4.2 beamline at ELETTRA (Trieste, Italy) [30]. The photon source is an electromagnetic elliptical wiggler that changes the helicity of the emitted photons reversing the current in its horizontal coils without mechanical movements of the magnetic arrays and changes in the optical axis. The beamline is equipped with two different monochromators that share the same entrance and exit slits: a normal incidence monochromator for the energy range 5–30 eV and a spherical grating monochromator in Padmore mount for the energy range 30–800 eV. In this work the exploited excitation energy range was 16–25 eV and 295–345 eV. The valence and core photoelectron spectra were recorded using two different experimental setups. In the valence setup the experimental chamber has two hemispherical analyzers set at 25 eV pass energy, with an overall resolution of about 250 meV. For the C 1s measurements we used a VG, 6-channeltrons, 150 mm hemispherical electron energy analyzer, set at 20 eV pass energy with an overall resolution of about 400 meV. A commercial S-(+)-isopropanolamine was purified by repeated sublimation cycles and admitted in the chamber in vapor phase through a needle, thermalized at 330 K, with an operative pressure of 5×10^{-6} mbar (the base pressure of the chambers was 5×10^{-7} mbar). The transmission of the electron analyzers and the binding energy calibration of the valence and core spectra were obtained by using the Ar 3p and C 1s CO_2 lines. The PECD measurements were taken reversing the photon helicity at 0.05 Hz, recording the two polarity branches of the spectrum at each kinetic energy point, in order to remove the drifts in the gas pressure and in the photon beam intensity.

A circular dichroism measure comes from the difference between spectral intensities taken with left and right circular polarized light. The differential photoelectron cross section with elliptical polarized light for a free chiral molecule is as follows [31]:

$$I \propto \frac{\sigma(\omega)}{4\pi}\left[1 - \frac{1}{2}\beta(\omega)P_2(\cos\theta_z) + \frac{3}{4}S_1(\omega)\beta(\omega)(\cos^2\theta_x - \cos^2\theta_y) + m_r S_3(\omega)D(\omega)P_1(\cos\theta_z)\right] \quad (1)$$

where $\sigma(\omega)$ is the isotropic photoelectron cross section, $\beta(\omega)$ is the asymmetry parameter and $D(\omega)$ is the dichroism parameter. In the expression (1) P_i refers to the Legendre polynomial of ith degree, S_1 and S_3 are the Stokes parameters relative to linear and circular light polarization vector components (normalized to the total intensity of the photon beam) [32], m_r is +1 or −1 for left and right circular polarization, θ_x, θ_y, θ_z are the angles composed by the photoelectron momentum and the Cartesian axis of the polarized light, where z is collinear with the propagation axis of the light, and y and x are the major and minor axis of the elliptically polarized light, respectively. The most suitable way of expressing D parameter is to plot it for each initial electronic state as a function of the photoelectron kinetic energy. In the valence band setup the two analyzers were set in forward-backward geometry, the first in the xz-plane at $\theta_z = 54.7°$ and $\theta_x = 35.3°$ (forward) and the second rotated by 180° along the y axis (backward). In the core level setup the VG analyzer was set in the forward geometry. These configurations ($\theta_z = 54.7°$ and $\theta_z = 234.7°$) ensure to have $P_2(\cos\theta_z) = 0$. To compare the experimental data with the theory, the D_{exp} parameter is expressed in the following way [14]:

$$D_{exp} = \frac{\sqrt{3}}{S_3}\frac{I^{(+)} - I^{(-)}}{I^{(+)} + I^{(-)}} \quad (2)$$

where $\sqrt{3}$ is the inverse of $P_1(\cos\theta_z)$ at $\theta_z = 54.7°$, $I^{(+)}$ and $I^{(-)}$ are the angular resolved photoelectron intensities for left and right circular polarization respectively.

The D_{exp} are calculated with the following procedure [10]: i) a fit performed for the unpolarized PES spectrum $[I^{(+)} + I^{(-)}]$ using Gaussian functions, ii) a fit performed for the difference PES spectrum $[I^{(+)} - I^{(-)}]$, employing the same energy positions and widths found for the unpolarized PES spectrum, iii) extraction of the D_{exp} parameter as a ratio of the area of each peak of the deconvoluted difference by the area of the corresponding peak of the unpolarized PES spectrum (see Eq. (2)). The fit parameters were optimized analyzing at the same time photoelectron spectra acquired at different photon excitation energies, exploiting the cross section intensity modulation to increase the significance of the deconvolution. The acquisition of PECD in forward-backward geometry allows us to take care of eventual systematic errors due to the alignment.

3. Computational details

The molecular structure of the two lowest energy conformers of isopropanolamine [33], named in the present work *I1* and *I2*, is displayed in Fig. 1. Isopropanolamine has a hydrogen bond between the hydroxyl (C—OH) and amino (C—NH_2) groups that locks free rotation of the molecule.

The geometric parameters and the molecular orbitals were derived by the ADF program [34], employing a density functional method with the Vosko-Wilk-Nusair (VWN) [35] local density approximation exchange correlation energy functional and a basis set of Slater type orbitals of double zeta plus polarization (DZP) type. The energy gap (from a single point Becke-Perdew [36,37] generalized gradient approximation calculation) of 4.80 kJ/mole between the two conformers is in agreement with previous estimates [33], giving at 330 K the ratio *I1*:*I2* as 1:0.18. The population relative to *I1* and *I2* represents the 91% of the total, and we assume the approximation of a two conformer population of *I1* and *I2* with percentage of 85% and 15%, respectively. The IE sequence for the two conformers was calculated by the outer-valence Green's

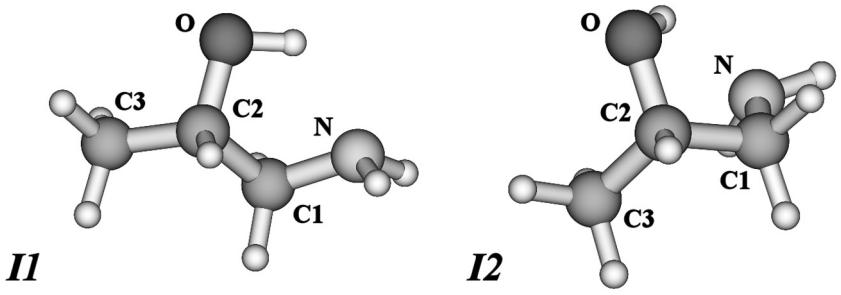

Fig. 1. Sketch of the calculated structures of the two conformers of S-(+)-isopropanolamine (*I1* and *I2*).

function (OVGF) [29] with Dunning cc-pVDZ basis set. The cross sections and the D parameters were obtained by a continuum calculation with the multicentric B-spline function approach [9]. The ground state density obtained from an SCF calculation employing the LB94 exchange-correlation potential with the same DZP basis set defines the Kohn-Sham (KS) Hamiltonian employed in continuum calculations. KS-LB94 ionization energies are listed in Table IV of Ref. [29].

It is worth noting that the exchange-correlation functional choice depends on the property of interest, so in this work we have employed VWN for the geometry, Becke-Perdew for the energetics, and LB94 for the calculation of the continuum. In particular LB94 is the only functional with the correct asymptotic behavior, which is very important for an accurate description of the continuum states. The role of vibrations on valence band PECD has been experimentally investigated for the HOMO of methyl oxirane at 22 eV of photon energy [22] with a smooth variation of the dichroic parameter across the vibronic structures of the order of 30% and at 10.4 eV [24] where the dichroism presents different signs. PECD data of methtyl-oxirane [11], measured with an experimental resolution that integrates the vibrational contribution, are in good agreement with the electronic DFT theory in the excitation range 12–70 eV. Indeed, the lack of a state of the art code that includes vibrational effect in the PECD hampers to assess if the relevant effect of vibrations should be confined in the low energy part of the PECD dispersion. However, from previous studies [11–15,25] we can consider electronic DFT theory a good starting point. The shape of the D_{exp} dispersions, obtained for each deconvoluted experimental photoelectron peak, is the result of different contributions due to the overlap of the electronic states of the conformers. The theoretical D dispersions take into account all these contributions, averaging the D values of *I1* and *I2* by the Boltzmann populations, used because it is not possible to disentangle the contributions of different conformers to the experimental photoelectron spectrum. Considering only the two most populated conformers, the average is defined as:

$$D_B(I) = \frac{\sum_n \sigma_{I1}^{(HOMO-n)} D_{I1}^{(HOMO-n)} (1 - e^{-\frac{\Delta E}{kT}}) + \sum_m \sigma_{I2}^{(HOMO-m)} D_{I2}^{(HOMO-m)} e^{-\frac{\Delta E}{kT}}}{\sum_n \sigma_{I1}^{(HOMO-n)} g_{I1}^{(HOMO-n)} (1 - e^{-\frac{\Delta E}{kT}}) + \sum_m \sigma_{I2}^{(HOMO-m)} g_{I2}^{(HOMO-m)} e^{-\frac{\Delta E}{kT}}} \quad (3)$$

where $D_B(I)$ for the Ith experimental deconvolved contribution is composed by the sum of the D theoretical parameters weighted by the specific conformer molecular orbital isotropic cross section (σ) and the Boltzmann population coefficient (ΔE is the calculated energy difference between the two conformers) [29] for each molecular orbital (HOMO-n, HOMO-m) that contributes to the deconvoluted peak. The normalization term contains the cross section and the *g* term, for the elliptical light contribution, defined as:

$$g_i(\beta, S_1, \theta_x) = 1 + \frac{3}{4}\beta_i S_1 \cos^2\theta_x \quad (4)$$

where β_i is the theoretical asymmetry parameter calculated for *I1* and *I2*. The *g* term, depending on S_1, β and θ_x, is used to take into account the effect of the elliptically polarized light and is related to the excess in intensity of linear polarized light in the x direction. This term and the specific conditions of our experiment do not affect significantly the normalization and the oscillatory behavior of data in terms of frequency and amplitude. The circularly polarized rate is obtained from calculation, and results in agreement with previous experiments. S_3 is 0.6 at 15 eV, 0.9 at 40 eV and 0.8 in the range 290–350 eV at storage ring electron energy 2.0 GeV. S_1 is calculated from the S parameters sum identity, since the unpolarized contribution is negligible in the source. The D_B, obtained from Eq. (3), directly relates to the D_{exp} parameter from the deconvoluted peak intensity.

4. Results and discussion

Fig. 2 reports the unpolarized photoelectron spectrum of isopropanolamine, measured at photon energy 22.5 eV (upper panel), and the relative difference spectrum acquired in forward direction (lower panel), together with the best fit generated using Voigt functions labeled with roman numerals. The molecular orbital IEs from the OVGF calculation for conformers *I1* and *I2* are represented by ticks in the upper panel of Fig. 2. The overall experimental error of the IE values was estimated about 50 meV. Since the OVGF IE difference for HOMO, HOMO-1 and HOMO-2 of the two conformers is less than the experimental resolution, we attribute the first three maxima of the photoelectron spectra at IE 9.55 eV (I), 10.40 eV (II), 11.60 eV (III) to a *I1* and *I2* Boltzmann average of the HOMO, HOMO-1, HOMO-2, respectively, and the shoulder at 12.6 eV (IV) to a *I1* and *I2* Boltzmann average of the HOMO-3. In the remaining IE region the comparison of the spectra features with the calculated IEs is not straightforward and we refer to Catone et al. [29] for the molecular orbital assignment. We allocate two Voigt components to the maximum at 13.24 eV (V) and to the shoulder at 13.87 eV (VI). The remaining deconvolved peaks are allocated one around the minimum in the photoelectron spectrum at IE 14.8 eV (VII), three in the band 14.8–17 eV (VIII, IX, X), and one clearly centered at IE 17.48 eV (XI). In Fig. 3 the theoretical dispersions of the D parameters as a function of the photoelectron kinetic energy for the two conformers (black and grey solid curves for *I1* and *I2* respectively) are presented for the valence molecular states from HOMO to HOMO-7. The theoretical D dispersions present different shapes for each conformer, confirming the sensitivity of PECD to structural changes.

Fig. 4 reports the D_{exp} for peak I and II as a function of the photoelectron kinetic energy, together with their respective D_B. The D_{exp} of peak I, assigned to HOMO:(*I1*, *I2*), is in fair agreement with the D_B dispersion, that reproduces quite well sign and order of magnitude of the experimental data. The effect of the second conformer is not appreciable because the maximum difference

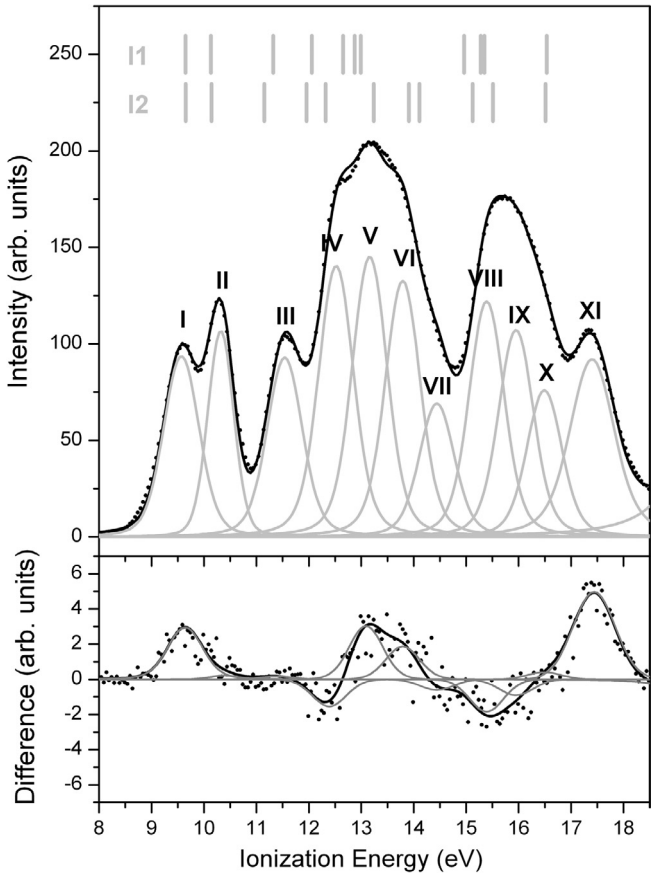

Fig. 2. Upper panel: unpolarized photoelectron spectrum of S-(+)-isopropanolamine measured at 22.5 eV of photon energy together with the best fit generated by Voigt functions, labeled with roman numerals; the ticks represent the IEs of the conformers calculated according to OVGF approximation [29]. Lower panel: Difference spectrum ($I^{(+)} - I^{(-)}$) (forward direction) together with the best fit generated using the same energy position and widths found for unpolarized spectrum.

between the theoretical dichroism of the Boltzmann average and of the most stable conformer is about 5%. The D_{exp} of peak II dispersion, related to the HOMO-1:(*I1*, *I2*), crosses the kinetic energy axis at 7.2 eV (interpolating linearly the data) in satisfactory agreement with the theory, that presents the zero cross at 8.6 eV.

Fig. 5 displays the experimental dispersions of peak III and IV, assigned to HOMO-2:(*I1*, *I2*) and HOMO-3:(*I1*, *I2*) respectively, together with the D_B curves as a function of the photoelectron kinetic energy. The theoretical dispersion related to peak III reproduces correctly the sign of the experimental data but fails in reproducing the shape of D_{exp} following an anti-phase behavior within the considered experimental kinetic energy range. The D_B curve related to the experimental peak IV has a qualitative resemblance in shape with the D_{exp} dispersion; the experimental minimum has the corresponding theoretical position shifted at 3.2 eV toward higher photoelectron energies, and the theory reproduces the sign only for the experimental point at 3.7 eV of kinetic energy.

To better understand how PECD can be affected by molecular structural changes, it is useful to compare the D_{exp} parameters of isopropanolamine and alaninol. We summarize from Ref. [29] the results of the conformer and electronic structure of alaninol and isopropanolamine and from Ref. [14] the results of alaninol PECD. The conformational population ratio of the two molecules (alaninol 68% A1:32% A2; isopropanolamine 85% I1:15% I2) has a predominant contribution of the lowest energy conformer. Table 1 presents the leading terms (based on heteroatoms) of the Mulliken population for HOMO and HOMO-1 calculated by KS-LB94 and HF. For both molecules KS-LB94 method composes HOMO as mainly due to O 2p and HOMO-1 to N 2p. HF and OVGF calculations in turn predict a different assignment: HOMO with a majority N 2p contribution and HOMO-1 with preponderant O 2p contribution, although the difference of the population is less pronounced than the KS-LB94 one. From the analysis of the HF and OVGF calculations, it is found that they give always the same ordering of the assignment of outer valence ionizations for both conformers of both molecules. The only exception refers to the inversion of the HOMO-5 and HOMO-6 pair of the *I1* conformer of isopropanolamine, which are, by the way, energetically very close each other (0.2 eV). For alaninol the D_B related to peak I shows an agreement in sign and magnitude with experimental data, whereas the D_B related to peak II has opposite sign with respect to the experiment and the accord in shape is only qualitative [14]. The discrepancy between experiment and theory for alaninol was attributed to a limit of the theoretical method to describe the electronic character of the HOMO and the HOMO-1.

Fig. 6 reports the D_{exp} dispersions of peak I–IV for isopropanolamine (black dots) and alaninol (grey dots) [14] as a function of photoelectron kinetic energy. The peaks I ÷ IV are related to HOMO ÷ HOMO-3, respectively, for both molecules. The peak I and peak II dispersions present similarities in sign, shape and order of magnitude for the two molecules in the experimental kinetic energy range considered. The two dispersions of peak I overlap up to 12 eV of photoelectron kinetic energy. The two dispersions of peak II share the same shape, but the isopropanolamine anticipates the minimum of about 2.5 eV of kinetic energy with respect to alaninol. The agreement between experiment and theory for the isopropanolamine peak I and II dispersions is more satisfactory than for alaninol [14]. From (i) the agreement of theory and experiment for HOMO and HOMO-1 of isopropanolamine, corroborating the KS-LB94 theoretical assignment, (ii) the close similarity of the HOMO and HOMO-1 experimental dispersions of the two molecules, (iii) the unsatisfactory comparison of KS-LB94 PECD calculations of HOMO and HOMO-1 dispersions of alaninol, we have hints to discuss the orbital assignment of alaninol. Point (i) and (iii) indicate that we should reconsider the validity of KS-LB94 HOMO and HOMO-1 orbital assignment of alaninol. Point (ii) suggests to consider the topological similarity in the spatial extension of the orbitals with respect to the skeleton structures of the two molecules. If we suppose that alaninol HOMO has a N 2p majority contribution, as predicted by HF and OVGF calculations, in a qualitative approach the analogies in both initial and final states could explain why the experimental dichroic dispersions are consistent. In the photoelectron emission process the initial state of the electron could be considered similar in the two molecules. In the final state the electron feels a potential that, by means of the analogy of the skeleton structure and of the functional groups, could also have a corresponding behavior in both molecules.

The shifted minimum in the D_{exp} of isopropanolamine peak II, shown in Fig. 6, could be attributed to slight changes in the molecular structure or in the potential. The presence of similarities in shape but not in energy position hampers the possible assignment of HOMO-1 of alaninol. Hence this analysis suggests that the alaninol HOMO should include a meaningful nitrogen 2p, as HF and OVGF calculations predict [29]. This heuristic argument confirms the extreme sensitivity of PECD to the character of the orbitals and to the structural properties of the chiral molecules.

The comparison of the D_{exp} dispersions of peaks III and IV of isopropanolamine and alaninol, assigned to HOMO-2 and HOMO-3 respectively (see Fig. 6), reveals a lack of similarities in shape, sign and intensity, that can be explained by the different electronic characters of these molecular orbitals, mainly due to the carbon atoms, and by the slight differences in the skeleton structures

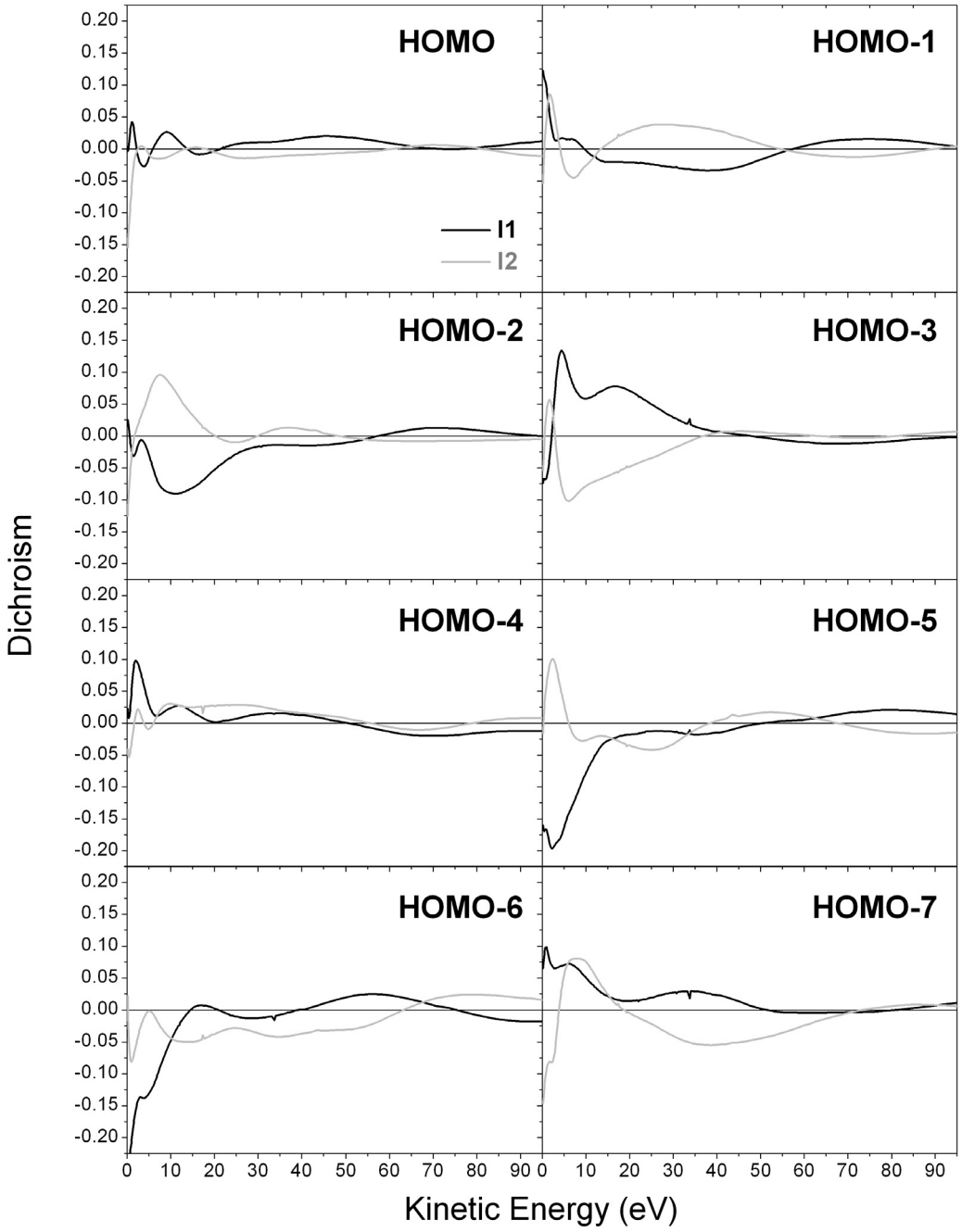

Fig. 3. Theoretical dispersion of D parameters as a function of photoelectron kinetic energy for the first eight valence states (from HOMO to HOMO-7) for the *I1* (black) and *I2* (grey) conformers of S-(+)-isopropanolamine.

[29]. The above discussion shows the advantages and drawbacks of PECD analysis. Important information on the electronic structure could stem from the direct comparison of the theoretical and experimental D dispersions of structural isomers. In particular for valence band this relation appears to be very significant in characterizing non-bonding states as lone pairs which play a fundamental role in the chemical reactivity and coordination. Classical techniques as absorption and photoelectron spectroscopy cannot reach the same sensitivity of PECD spectroscopy because the characteristic features in the spectra slightly changes or are not clearly related upon tiny differences in the electronic structure. However, the investigation of classes of molecules by PECD, relating electronic and structural properties to the shape of the D experimental dispersion, should improve the experimental methods, measuring a wider range of excitation energies to better compare the shape of the dispersions, and include in the theory effects of vibrations and rotations. In view of these considerations, our works does not solve completely the attribution of the HOMO and HOMO-1 of alaninol and isopropanolamine, as expected in the conclusions of Ref. [29], but indicates on the ground of the comparison between experiments and theory a possible path for a further investigation. In Fig. 7 the D_{exp} and D_B dispersions of the peaks V ÷ VII are reported as a function of photoelectron kinetic energy. The peak V of isopropanolamine, assigned to HOMO-4:(*I1*, *I2*), presents a dispersion with a maximum at 6.9 eV, and is reproduced qualitatively by the D_B curve in sign, order of magnitude and shape, presenting the maximum shifted of 4.8 eV toward higher kinetic energies. The peak VI dispersion, attributed to HOMO-5:(*I1*, *I2*) and HOMO-6:

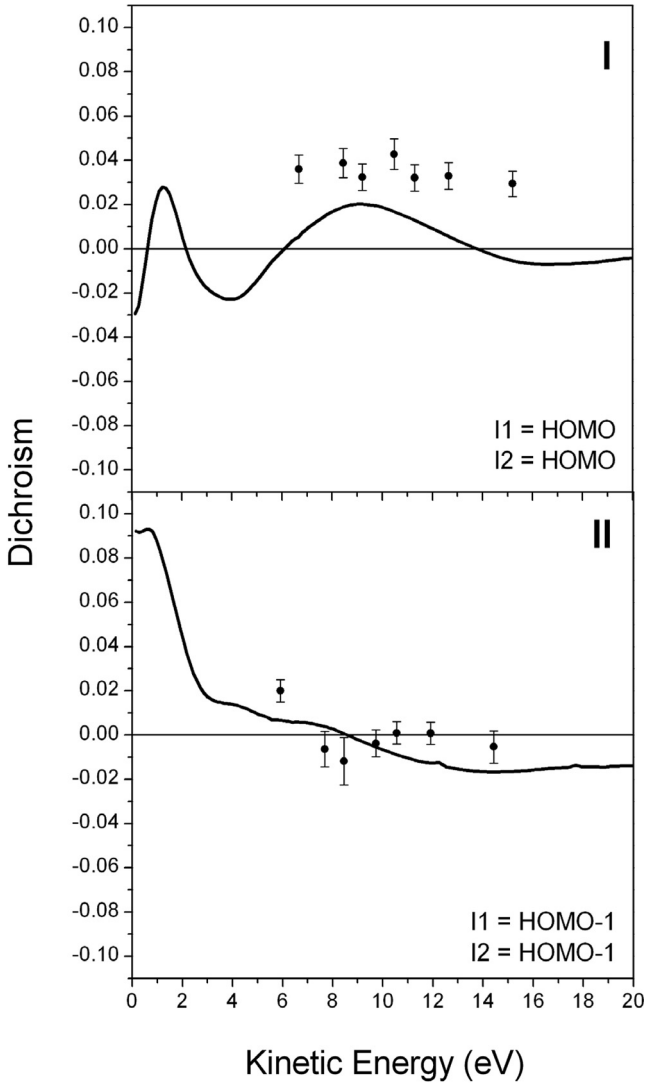

Fig. 4. Valence D_{exp} of peak I and peak II (dots) as a function of the photoelectron kinetic energy together with the related D_B dispersions (solid curve), generated considering the populations of the two conformers of S-(+)-isopropanolamine.

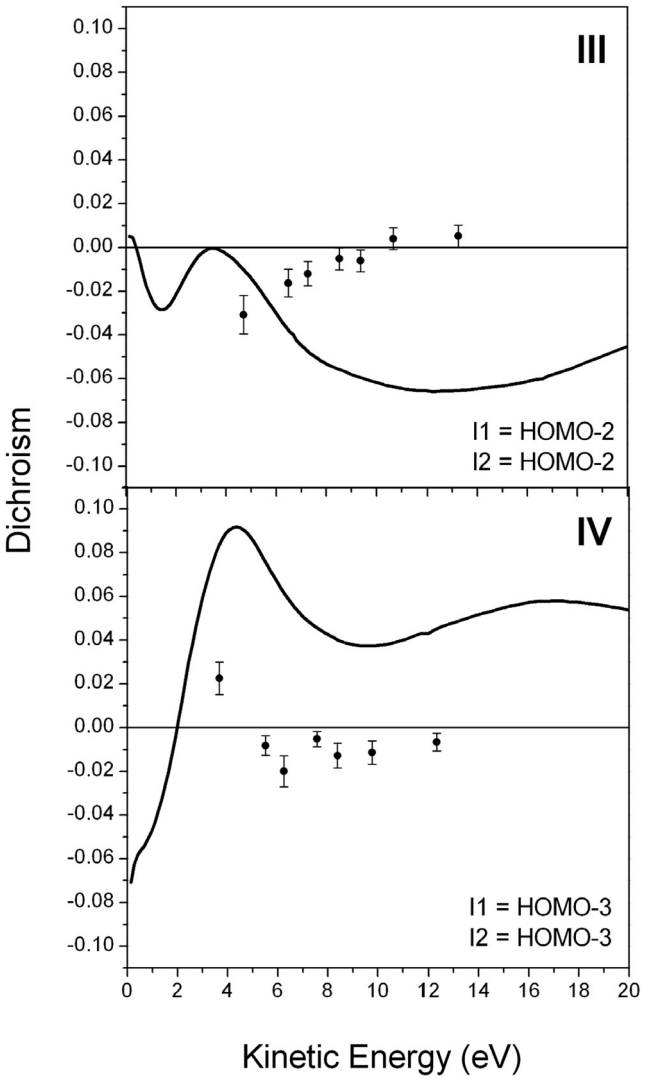

Fig. 5. Valence D_{exp} of peak III and peak IV (dots) as a function of the photoelectron kinetic energy together with the related D_B dispersions (solid curve), generated considering the populations of the two conformers of S(+)-isopropanolamine.

(*I1*), has a qualitative agreement in shape with the D_B curve, even if its inflection point is shifted at about 7 eV toward higher kinetic energies. The peak VII dispersion of isopropanolamine is assigned by the OVGF calculation to HOMO-6:(*I2*) and HOMO-7:(*I2*) contributions, related only to the less abundant conformer *I2*. The presence of a strong dichroism in the dispersion at 1.6 eV provides evidence for the presence of states lying near the minimum at IE 14.8 eV of the photoelectron spectrum that are consistent with the OVGF prediction and with the shape of the photoelectron spectrum. It is probable that in the proposed deconvolution there is a contribution of tails of states of the prevalent conformer, not represented in the proposed assignment, which can distort the comparison; however the OVGF ionization energy assignment, that places the HOMO-6:(*I2*) and HOMO-7:(*I2*) in an IE region not overlapping *I1* orbitals, and the experimental D dispersion are consistent with the *I2* contribution. Moreover, a similar contribution of the population of the minority conformer in the PECD dispersion was observed in alaninol PECD for HOMO-4 [14]. In this case it is worth to underline the complementary nature of the two spectroscopies to assign the electronic properties to a single conformational contribution.

The comparison between theory and experiment reveals only a qualitative agreement with the proposed assignments. The main limit in this analysis is the deconvolution procedure in absence of definite features in the PES and PECD spectra, the grouping of the molecular orbitals according to a theoretical calculation and the high correlation of the parameters in the fit analysis, that makes difficult to disentangle small contributions. Nonetheless, despite these very crude approximations, the analysis shows a qualitative agreement with the relevant information of the calculated electronic and structural properties of the molecules.

Fig. 8 reports the experimental C 1s photoelectron spectrum measured at 310 eV of photon energy, together with the best fit generated using two Gaussian functions. We assign the lower IE feature of the spectrum (peak A) to the carbon methyl group, and the main peak (peak B) to the unresolved contribution of the two carbon atoms bound to the hydroxyl and amino groups. Fig. 9 shows the D_{exp} dispersions of peak A and peak B, together with the related D_B curves as a function of photoelectron kinetic energy. The D_{exp} dispersions are measured in the kinetic energy range of 3–50 eV and the maximum intensity revealed is about 0.03. In both cases the D_B curves reproduce the experimental data with good accuracy. The maximum in the first oscillation of the dispersion

Table 1
Calculated KS-LB94 and Hartree-Fock molecular orbital Mulliken population of alaninol *A1* conformer, and isopropanolamine *I1* conformer [29].

MO	KS-LB94		Hartee-Fock	
	A1	I1	A1	I1
HOMO	57% O 2p, 11% N2p	50% O 2p, 15% N 2p	43% N 2p, 22% O 2p	37% N 2p, 24% O 2p
HOMO-1	52% N 2p, 14% O 2p	48% N 2p, 18% O 2p	36% O 2p, 24% N 2p	31% O 2p, 29% N 2p

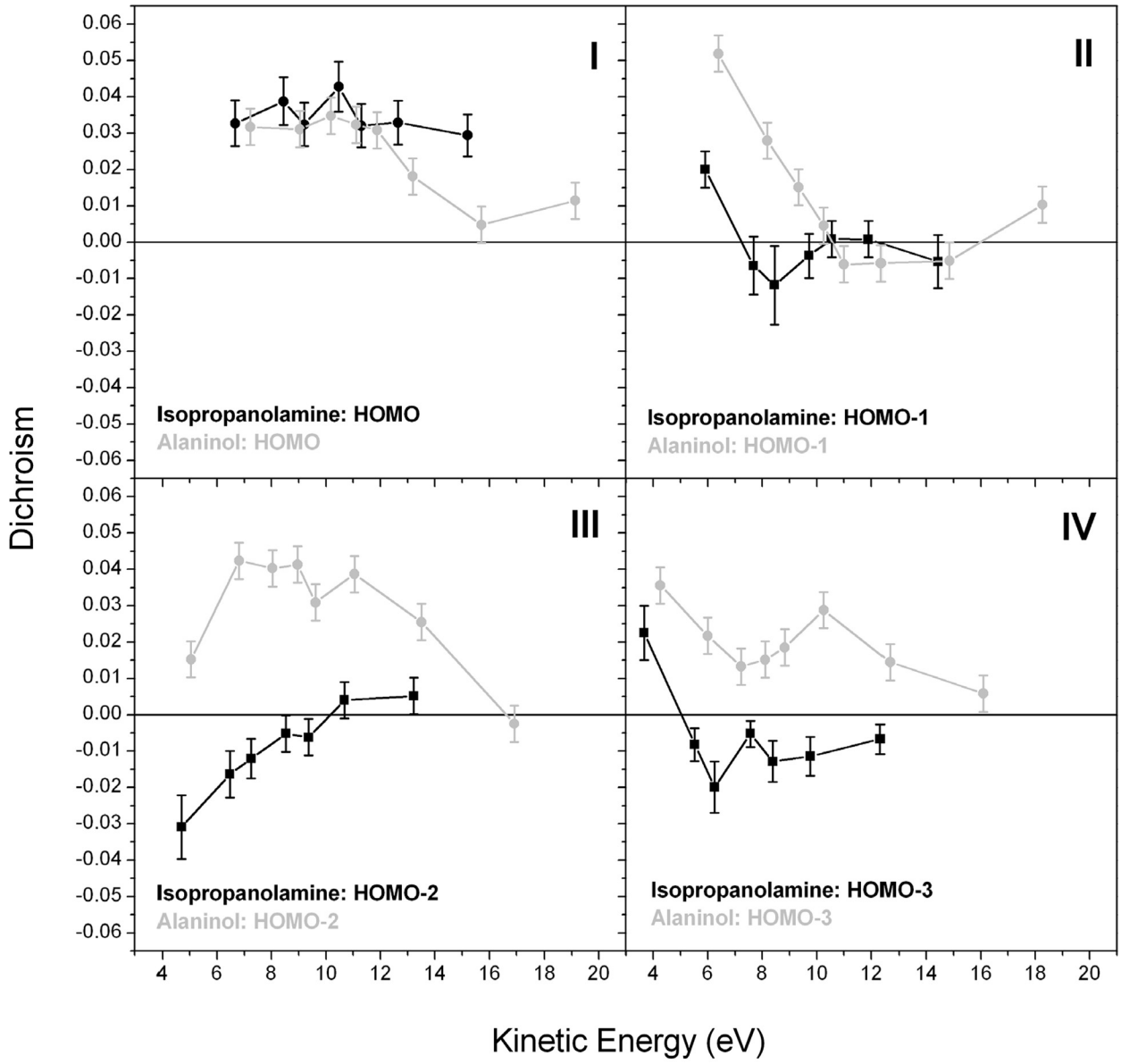

Fig. 6. Valence D_{exp} of peak I–IV as a function of the photoelectron kinetic energy of S-(+)-isopropanolamine (black dots) and S-(+)-alaninol [14] (grey dots).

of peak A is reproduced with a shift of about 5 eV toward lower kinetic energies. The D_{exp} of peak B is well reproduced by theory in the whole spectrum. The flexibility of the methyl group with respect to the oxydrilic and amino groups could explain the different level of correspondence [20]. The core level orbitals are mostly based on C1s wavefunction, then the s character of the initial state limits the number of angular momentum channels which give non zero dipole matrix elements. A simple analysis can be performed writing the wavefunction of the photoemitted electron state in a monocentric expansion around the C absorber as:

$$\psi_{lm}^{(-)} \propto \sum_{l'm'} R_{lm,l'm'}(r) Y_{l'm'}(\vartheta,\phi)$$

where the angles ϑ, ϕ specify the direction of r in the laboratory frame. The partial waves satisfy incoming boundary conditions. The R term depends on l and l' since the partial waves are mixed by the molecular potential. Considering C 1s as the most relevant term of the initial state, the dipole selection rules allows only $R_{lm,1m'}(r)$ contributions. A pure 1s orbital is an eigenfunction of the magnetic dipole operator with eigenvalue zero and the intensity

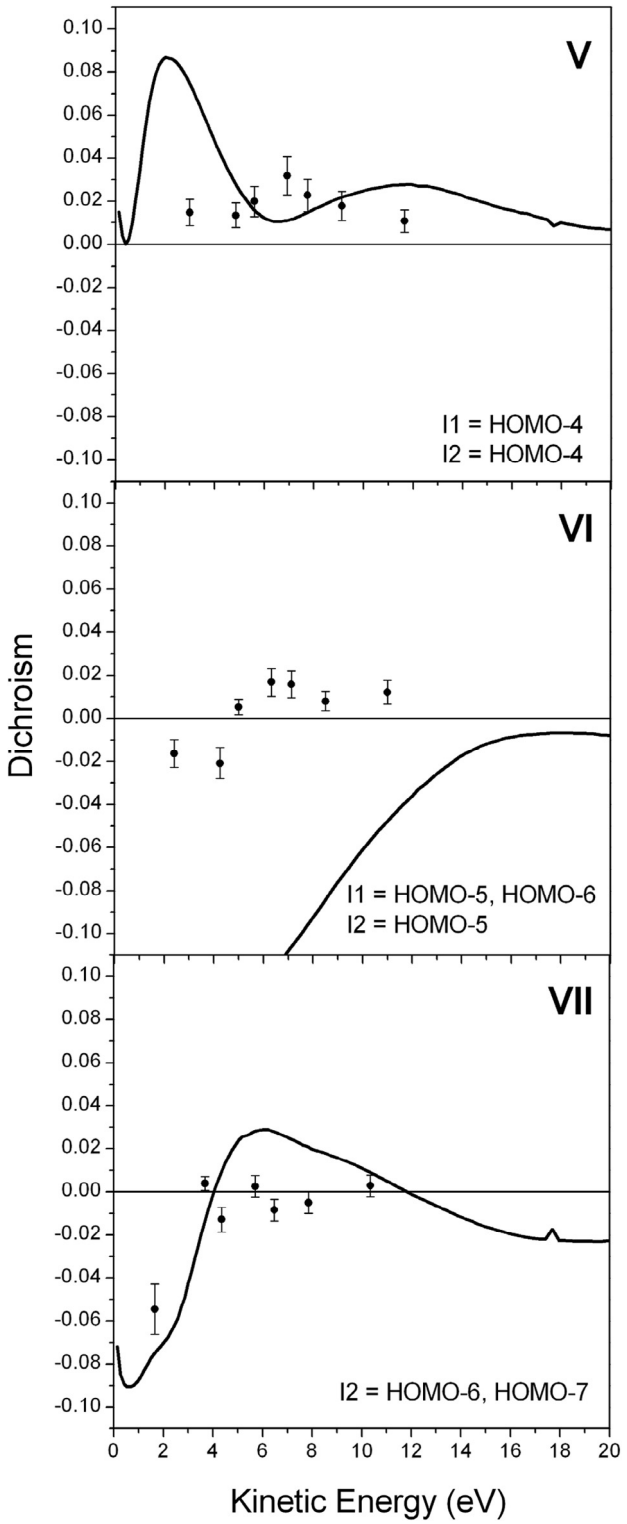

Fig. 7. Valence D_{exp} of peak V–VII (dots) as a function of the photoelectron kinetic energy together with the related D_B dispersions (solid curve), generated considering the populations of the two conformers of S-(+)-isopropanolamine.

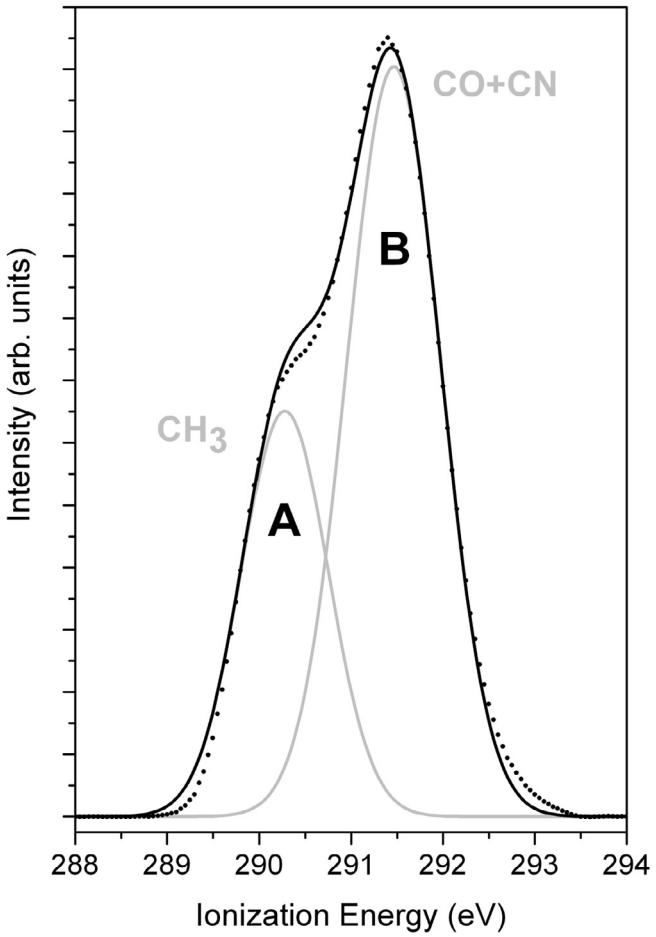

Fig. 8. C 1s photoelectron spectrum of S(+)-isopropanolamine measured at 310 eV of photon energy, together with the best fit generated using two Gaussian functions, labeled A and B.

of circular dichroism in absorption is null. The different level of agreement between theory and experiments in the valence and the core states stems from the extreme sensitivity of the PECD signal to the electronic structure. In the core state, the calculation reproduces better the measured intensity since the initial state is very sharply defined and the final state wavefunction is probed locally and in a reduced number of channels. The localization of the core level D parameter does not hinder the determination of the absolute configuration of the enantiomer and the sensitivity to structural properties of the whole molecule [38]. The success of the DFT theory in reproducing the core level PECD of the two carbon atoms bound to the hydroxyl and amino groups, located in the moiety of the molecule where HOMO and HOMO-1 are mainly located, reveals the importance of a correct initial state in PECD calculations.

5. Conclusions

This work reports on the comparison between experiment and theory of the photoelectron spectroscopy circular dichroism for S-(+)-isopropanolamine. The agreement of the experimental and theoretical D_B photoelectron kinetic energy dispersions of HOMO and HOMO-1 is reasonably satisfactory, with correct sign, order of magnitude and shape. Comparing the experimental HOMO D_{exp} dispersions of isopropanolamine and alaninol an important resemblance was found, proving that similar electronic and structural properties can lead a similar behavior in the D_{exp} dispersion. The 2p atomic electronic character and the topological similarity for the spatial extension of the molecular orbital with respect to the skeleton structure is a valid argument to justify the close analogies between the HOMO D_{exp} dispersions. Classical techniques as absorption and photoelectron spectroscopy cannot reach the same

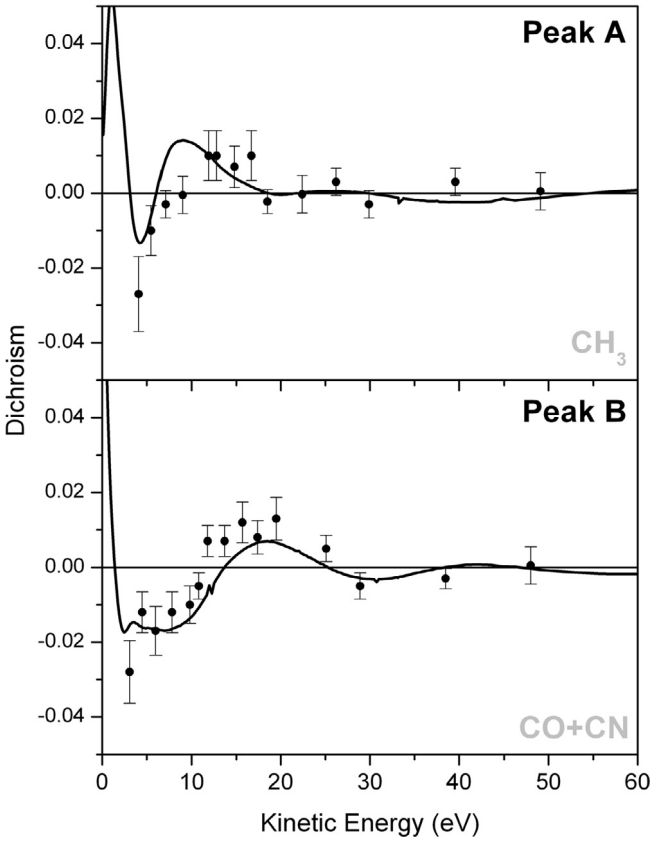

Fig. 9. D_{exp} of peak A and peak B (dots) as a function of the photoelectron kinetic energy together with the related D_B dispersions (solid curve), generated considering the populations of the two conformers of S-(+)-isopropanolamine.

sensitivity of PECD spectroscopy because of the higher interferential nature of the D parameter. PECD confirms the OVGF assignment of the conformational *I2* electronic contributions to peak VII, revealing the presence of states that cannot be associated to pronounced features of the PES spectrum.

Discrepancies found for innermost ionizations can be traced both on incomplete band resolution due to orbital congestion and to inadequate initial state representation by DFT orbitals, as well as from conformational flexibility.

Further studies on different classes of molecules are needed to precisely understand the interplay between electronic structure and molecular geometry. This work shows that investigating class of molecules that share some electronic and structural properties is a powerful tool for a deep understanding of the fundamentals of the PECD. The C 1s core level PECD study confirms an excellent agreement with B-spline DFT theory, showing the potential applications for local electronic and structural properties.

References

[1] K.T. Wan, M.E. Davis, Nature 370 (1994) 449.
[2] K.-H. Ernst, Phys. Status Solidi B 249 (2012) 2057.
[3] S. Irrera, G. Contini, N. Zema, S. Turchini, J. Fujii, S. Sanna, T. Prosperi, J. Phys. Chem. B 111 (2007) 7478.
[4] G. Contini, P. Gori, F. Ronci, N. Zema, S. Colonna, M. Aschi, A. Palma, S. Turchini, D. Catone, A. Cricenti, T. Prosperi, Langmuir 27 (2011) 7410.
[5] B. Ritchie, Phys. Rev. A 13 (1976) 1411.
[6] N. Böwering, T. Lischke, B. Schmidtke, N. Müller, T. Khalil, U. Heinzmann, Phys. Rev. Lett. 86 (2001) 1187.
[7] U. Hergenhahn, E.E. Rennie, O. Kugeler, S. Marburger, T. Lischke, I. Powis, G. Garcia, J. Chem. Phys. 120 (2004) 4553.
[8] I. Powis, J. Chem. Phys. 112 (2000) 301.
[9] M. Stener, G. Fronzoni, D.D. Tommaso, P. Decleva, J. Chem. Phys. 120 (2004) 3284.
[10] S. Turchini, N. Zema, G. Contini, G. Alberti, M. Alagia, S. Stranges, G. Fronzoni, M. Stener, P. Decleva, T. Prosperi, Phys. Rev. A 70 (2004) 14502.
[11] S. Stranges, S. Turchini, M. Alagia, G. Alberti, G. Contini, P. Decleva, G. Fronzoni, M. Stener, N. Zema, T. Prosperi, J. Chem. Phys. 122 (2005) 244303.
[12] M. Stener, D. Di Tommaso, G. Fronzoni, P. Decleva, I. Powis, J. Chem. Phys. 124 (2006) 024326.
[13] A. Giardini, D. Catone, S. Stranges, M. Satta, M. Tacconi, S. Piccirillo, S. Turchini, N. Zema, G. Contini, T. Prosperi, P. Decleva, D. Di Tommaso, G. Fronzoni, M. Stener, A. Filippi, M. Speranza, ChemPhysChem 6 (2005) 1164.
[14] S. Turchini, D. Catone, G. Contini, N. Zema, S. Irrera, M. Stener, D. Di Tommaso, P. Decleva, T. Prosperi, ChemPhysChem 10 (2009) 1839.
[15] S. Turchini, D. Catone, N. Zema, G. Contini, T. Prosperi, P. Decleva, M. Stener, F. Rondino, S. Piccirillo, K.C. Prince, M. Speranza, ChemPhysChem 14 (2013) 1723.
[16] C.J. Harding, E. Mikajlo, I. Powis, S. Barth, S. Joshi, V. Ulrich, U. Hergenhahn, J. Chem. Phys. 123 (2005) 234310.
[17] I. Powis, C.J. Harding, S. Barth, S. Joshi, V. Ulrich, U. Hergenhahn, Phys. Rev. A 78 (2008) 052501.
[18] A.G. Garcia, L. Nahon, C.J. Harding, I. Powis, Phys. Chem. Chem. Phys. 10 (2008) 1628.
[19] G.A. Garcia, H. Soldi-Lose, L. Nahon, I. Powis, J. Phys. Chem. A 114 (2010) 847.
[20] D. Di Tommaso, M. Stener, G. Fronzoni, P. Decleva, ChemPhysChem 7 (2006) 924.
[21] I. Powis, Adv. Chem. Phys. 138 (2008) 267.
[22] G. Contini, N. Zema, S. Turchini, D. Catone, T. Prosperi, V. Carravetta, P. Bolognesi, L. Avaldi, V. Feyer, J. Chem. Phys. 127 (2007) 124310.
[23] I. Powis, Phys. Rev. A 84 (2011) 013402.
[24] G.A. Garcia, L. Nahon, S. Daly, I. Powis, Nat. Commun. 4 (2013) 2132.
[25] D. Catone, M. Stener, P. Decleva, G. Contini, N. Zema, T. Prosperi, V. Feyer, K.C. Prince, S. Turchini, Phys. Rev. Lett. 108 (2012) 083001.
[26] J.W. Kim, M. Carbone, J.H. Dil, M. Tallarida, R. Flammini, M.P. Casaletto, K. Horn, M.N. Piancastelli, Phys. Rev. Lett. 95 (2005) 107601.
[27] G. Contini, S. Turchini, S. Sanna, D. Catone, J. Fujii, I. Vobornik, T. Prosperi, N. Zema, Phys. Rev. B 86 (2012) 035426.
[28] M.M.R. Fanood, N.B. Ram, C.S. Lehmann, I. Powis, M.H.M. Janssen, Nat. Commun. 6 (2015) 7511.
[29] D. Catone, S. Turchini, G. Contini, N. Zema, S. Irrera, T. Prosperi, M. Stener, D. Di Tommaso, P. Decleva, J. Chem. Phys. 127 (2007) 144312.
[30] D. Desiderio, S. Di Fonzo, B. Diviacco, W. Jark, J. Krempasky, R. Krempaska, F. Lama, M. Luce, H.-C. Mertins, M. Piacentini, T. Prosperi, S. Rinaldi, G. Soullie, F. Schäfers, F. Schmolle, L. Stichauer, S. Turchini, R.P. Walker, N. Zema, Synchrotron Radiat. News 12 (1999) 34.
[31] J.A.R. Samson, A.F. Starace, J. Phys. B Atom. Mol. Phys. 8 (1975) 1806.
[32] M. Born, E. Wolf, Principles of Optics, Pergamon, New York, 1959.
[33] C. Cacela, R. Fausto, M.L. Duarte, Vibr. Spectrosc. 26 (2001) 113.
[34] E.J. Baerends, D.E. Ellis, P. Ros, Chem. Phys. 2 (1973) 41.
[35] S.H. Vosko, L. Wilk, M. Nusair, Can. J. Phys. 58 (1980) 1200.
[36] A.D. Becke, Phys. Rev. A 38 (1988) 3098.
[37] J.P. Perdew, Phys. Rev. B 33 (1986) 8822.
[38] V. Ulrich, S. Barth, S. Joshi, U. Hergenhahn, E. Mikajlo, C.J. Harding, I. Powis, J. Phys. Chem. A 112 (2008) 3544–3549.